Experimental and Molecular Pathology 145 (2026) 105025

Contents lists available at ScienceDirect

Experimental and Molecular Pathology

journal homepage: www.elsevier.com/locate/yexmp

Metixene hydrochloride hydrate mitigates kidney tubulointerstitial fibrosis by inhibiting Smad3 phosphorylation☆

Kyeong-Min Lee [a,1,*], Yeo Jin Hwang [b,1]

[a] Division of Biomedical Technology, Daegu Gyeongbuk Institute of Science and Technology, Daegu 42988, Republic of Korea
[b] Division of AI, Big Data and Block Chain, Daegu Gyeongbuk Institute of Science and Technology, Daegu 42988, Republic of Korea

ARTICLE INFO

Keywords:
Metixene
Chronic kidney disease
Renal fibrosis
Transforming growth factors
Smad3
Unilateral ureteral obstruction

ABSTRACT

Chronic Kidney disease (CKD), in which renal fibrosis is the defining pathological feature, poses significant global health and economic challenges. Despite its high clinical prevalence, effective therapies to prevent or reverse renal fibrosis remain scarce. Metixene hydrochloride hydrate (MHH), an anticholinergic drug once used for Parkinson's disease, has not been evaluated for renal fibrosis. Here, we investigated whether MHH mitigates renal fibrosis in a unilateral ureteral obstruction (UUO) mouse model and evaluated its effects on transforming growth factor-β1 (TGF-β1) signaling in renal cells. MHH did not affect the cell viability of NRK-49F cells at concentrations ranging from 0.5 to 5 μM. In vitro, MHH effectively suppressed TGF-β1-induced PAI-1 expression (both mRNA and protein) and secretion in renal fibroblasts, as well as PAI-1 secretion and protein expression in renal glomerular endothelial cells. Furthermore, TGF-β1 stimulated the mRNA and protein expressions of key renal fibrotic factors, including collagen type I, fibronectin, and alpha-smooth muscle actin, in NRK-49F cells. MMH significantly inhibited the expression of these renal fibrotic factors in these cells. UUO kidneys exhibited markedly increased tubular atrophy and interstitial fibrosis, as well as increased expression of renal fibrotic markers. MHH treatment significantly mitigated these pathological parameters and expression of renal fibrotic markers. Mechanistically, MHH suppressed TGF-β1-induced Smad3 phosphorylation both in vitro and in vivo. Our findings indicate that MHH exerts potent antifibrotic effects by downregulating the TGF-β1/Smad3 signaling pathway and suppressing the expression of fibrotic factors in renal cells and obstructed kidneys. Therefore, MHH could be repositioned as a therapeutic agent for renal fibrosis in various kidney diseases.

1. Introduction

Chronic kidney disease (CKD) is characterized by persistent renal dysfunction and a progressive decline in kidney function, ultimately resulting in irreversible renal failure (Levey and Coresh, 2011; Ruiz-Ortega et al., 2020). Eventually, it progresses to end-stage renal disease (ESRD), necessitating kidney replacement therapies including dialysis or transplantation, which are associated with severe pain, increased risk of mortality, and substantial financial burden for the patient (Lv and Zhang, 2019; Orr and Bridges, 2017). The global prevalence of CKD (stages 1–5) is estimated to be approximately 13.4%, affecting over 800 million individuals (Duff et al., 2024; Hill et al., 2016). Furthermore, its mortality burden is rapidly increasing; CKD has risen to become one of the top ten leading causes of death globally (Feng et al., 2023; Guo et al., 2025). Renal fibrosis is a prominent pathological feature and a significant risk factor for progressive CKD, characterized by abnormal accumulation of ECM within kidney tissue, tubulointerstitial structural deterioration, and fibroblast proliferation (Hodgkins and Schnaper,

Abbreviations: CKD, Chronic kidney disease; ESRD, end-stage renal disease; TGF-β1, transforming growth factor-beta1; PAI-1, plasminogen activator inhibitor-1; MHH, metixene hydrochloride hydrate; UUO, unilateral ureteral obstruction; α-SMA, alpha-smooth muscle actin; GAPDH, glyceraldehyde 3-phosphate dehydrogenase; CCK-8, cell counting kit-8; qPCR, quantitative polymerase chain reaction; ELISA, enzyme-linked immunosorbent assay; H&E, hematoxylin and eosin; SEM, standard error of the mean.

☆ This article is part of a Special issue entitled: 'EMP – Metabolism' published in Experimental and Molecular Pathology.

* Corresponding author at: Division of Bimedical Technology, Daegu Gyeongbuk Institute of Science and Technology, 333 Techno Jungang Daero, Hyeonpung-Eup, Dalseong-Gun, Daegu 42988, Republic of Korea.
E-mail address: leekm1009@dgist.ac.kr (K.-M. Lee).

[1] Kyeong-Min Lee and Yeo Jin Hwang have contributed equally to this study as the first author.

https://doi.org/10.1016/j.yexmp.2026.105025
Received 28 August 2025; Received in revised form 9 January 2026; Accepted 9 January 2026
Available online 16 January 2026

2012; Huang et al., 2023; Li et al., 2022). Currently, there are few effective therapeutic options for renal fibrosis. Therefore, identifying novel agents that can effectively control renal fibrosis and elucidating their underlying mechanisms may facilitate the development of new therapeutic strategies or, at least, delay renal deterioration.

Among the molecular drivers of renal fibrosis, transforming growth factor-beta1 (TGF-β1) plays a pivotal role by activating Smad dependent signaling, particularly through the phosphorylation of Smad3 (Ma and Meng, 2019; Ren et al., 2023; Zou et al., 2025), which promotes fibroblast activation, and ECM production (Gu et al., 2024; Zou et al., 2025), including plasminogen activator inhibitor-1 (PAI-1), collagen type I and fibronectin (Chia et al., 2024; Lee et al., 2024; Yu et al., 2003)Excessive ECM deposition in kidney tissue is recognized as a common pathological feature of CKD that leads to the development of end-stage renal disease, accompanied by a progressive renal dysfunction (Ruiz-Ortega et al., 2020; Sobreiro-Almeida et al., 2021). Therefore, targeting the TGF-β1/Smad3 axis has emerged as a promising therapeutic strategy to mitigate renal fibrosis in both diabetic and non-diabetic settings (Gagliardini and Benigni, 2007; Gifford et al., 2021; Zhang et al., 2018).

Drug repurposing, identifying new therapeutic uses for existing drugs originally developed for other indications, is a novel strategy for expanding treatment options. This approach accelerates the discovery of novel therapies by leveraging the established safety profiles and pharmacological data of approved drugs (Li and Jones, 2012; Würth et al., 2016). In this study, we screened FDA-approved agents in renal cells to identify inhibitors of TGF-β-induced PAI-1 secretion. We identified metixene hydrochloride hydrate (MHH), an anticholinergic compound previously approved for treating Parkinsonian syndromes (Scott and Njardarson, 2019), as a potent inhibitor of renal fibrosis. Additionally, MHH has recently been proposed as a therapeutic agent for primary breast cancer brain metastases (Fares et al., 2023). However, the effects of MHH on renal fibrosis have not been thoroughly investigated.

In this study, we evaluated the antifibrotic potential of MHH in TGF-β1-stimulated NRK-49F cells and a mouse model of UUO. Our results demonstrate that MHH significantly attenuates fibrotic responses and inhibits Smad3 phosphorylation, indicating that MHH may serve as a promising repositioned drug for treating renal fibrosis associated with diabetes.

2. Materials and methods

2.1. UUO model and drug administration

Male C57BL/6 (8–10 week-old, 25 ± 2 g) mice were purchased from the Koatech Technology Corporation (Pyeongtaek-si, Korea) and were bred under standard room temperature (22 ± 2 °C) and humidity (60 ± 10%) with a 12 h light/dark cycle. MHH (MedchemExpress, Monmouth, NJ, USA) for oral treatment was dissolved in filtered solution (1.25% dimethyl sulfoxide (DMSO), 2% polyethylene glycol 400, 0.5% Tween 20 in saline). Mice were randomly assigned to four experimental groups ($n = 7$ per group): Sham (vehicle), Sham+MHH (MHH, 5 mg/kg/day), UUO (vehicle), and UUO + MHH (MHH, 5 mg/kg/day). Five days prior to the UUO operation, animals in the MHH groups were orally pretreated by gavage with MHH in equivalent volumes to the vehicle group. Mice were anesthetized via intraperitoneal (IP) injection of xylazine (10 mg/kg) and ketamine (100 mg/kg), and unilateral ureteral obstruction (UUO) was performed by ligating the left ureter (Lee et al., 2024; Jung et al., 2020) for 10 days. Sham-operated mice served as controls. Upon completion of the experimental period, mice were anesthetized for blood collection and subsequently kidney tissue harvesting following transcardial perfusion with PBS. All animal experiments were approved by the Animal Care and Use Committee of Daegu Gyeongbuk Institute of Science and Technology (DGIST-IACUC-19052105-01)

2.2. Cell culture

Kidney interstitial fibroblasts (NRK—49F, ATCC, CRL-1570, Manassas, VA, USA) were cultured in Dulbecco's Modified Eagle Medium /Nutrient Mixture F-12 medium (Gibco, 11320033, Waltham, MA, USA) supplemented with 10% fetal bovine serum, 100 U/mL penicillin, and 100 μg/mL streptomycin (Welgene, Gyeongsan-si, Korea). Renal glomerular endothelial cells (Innoprot, P10665, Derio, Bizkaia, Spain) were cultured in Endothelial Cell Medium Kit (Innoprot, P60104). Cells were maintained at 37 °C in a humidified incubator with 5% CO_2. MHH was dissolved in DMSO and diluted to final concentrations of 1–5 μM for treatment. Recombinant human TGF-β1 (R&D Systems, #240-B, Minneapolis, MN, USA) was used at 2 ng/mL to induce fibrotic responses.

2.3. Cell viability assay

Cell viability was assessed using a D-PlusTM CCK cell viability assay kit (Dongin, CCK-5000, Seoul, Korea). NRK-49F cells were seeded in 96-well plates, cultured for 24 h, and subsequently treated with MHH (1–10 μM) for an additional 24 h. Absorbance was measured at 450 nm using a microplate reader, and cell viability was expressed as a percentage of control values.

2.4. Reporter assay

NRK49-F cells were seeded in 12-well plates and cultured for 24 h. Cells were transiently transfected with the PAI-1 promoter construct for 4 h using Lipofectamine2000 (Thermo Scientific, 11668019, Waltham, MA, USA), then washed to remove unincorporated plasmids. Transfected cells were incubated with 2 ng/mL TGF-β1 for 24 h in the presence of the indicated concentrations of MHH. Cells were harvested 24 h after transfection and then measured for luciferase activity using a GloMax navigator (Promega, Madison, WI, USA).

2.5. ELISA for PAI-1

NRK-49F cells (4×10^3/well) or renal glomerular endothelial cells (3×10^3/well) were seeded in a 96-well plate and cultured for 24 h. Cells were incubated in medium containing 0.5% FBS for 24 h and then treated with TGF-β1 (2 or 5 ng/mL) with or without MHH (0–5 μM) for an additional 24 h. Supernatants were collected, and secreted PAI-1 levels were quantified using a commercial ELISA kit (Abcam, ab201283, Cambridge, UK) according to the manufacturer's instructions.

2.6. Western blot analysis

Proteins were extracted using RIPA lysis buffer (Thermo Scientific, 89900) containing cOmpleteTM, Mini Protease Inhibitor Cocktail (Roche, 11836153001, Basel, Switzerland), and Halt Phosphatase Inhibitor Cocktail (Thermo Scientific, 78420). Equal amounts of protein were separated by Mini-PROTEAN® Gels (Bio-Rad, 4561025, Hercules, CA, USA), transferred to polyvinylidene difluoride membranes (Bio-Rad), and probed with primary antibodies; anti-collagen type I (1:500, ab138492, Abcam), anti-fibronectin (1:1000, ab2413, Abcam), anti-alpha-smooth muscle actin (α-SMA, 1:1000, 610620, BD Biosciences, Franklin Lakes, NJ, USA), anti-PAI-1 (1:500, 612024, BD Biosciences), anti-phospho-Smad3 (1:500, Cell Signaling, 9520, Danvers, MA, USA) and anti-glyceraldehyde 3-phosphate dehydrogenase (GAPDH, 1:1000, Santacruz, sc-32233, Dallas, TX, USA). Bands were visualized using ChemiDoc TMXRS+ (Bio-Rad) and quantified using Image J software 1.53e (National Institutes of Health, Bethesda, MD, USA).

2.7. Quantitative real-time PCR (qRT-PCR)

Total RNA was extracted from cells and renal tissues using RNA

extraction kits (Takara, 740948.50, Tokyo, Japan). cDNA was synthesized using a reverse transcription kit (Applied Biosystems, 4368814, Waltham, MA, USA). qRT-PCR was performed using SYBR Green Master Mix (Applied Biosystems, 4309155) on an ABI 7500 qPCR system, and gene expression was normalized to GAPDH. Primer sequences for collagen I alpha 1, PAI-1, fibronectin, and α-SMA were previously described (Lee et al., 2024) and provided in Table S1.

2.8. Histological analysis and immunohistochemical staining

Kidneys were fixed in a formalin solution (Sigma-Aldrich, HT50165, Burlington, MA, USA), embedded in paraffin, and then sectioned. Hematoxylin and eosin (H&E) and Sirius Red staining were performed to assess tubular damage and fibrosis. Fibrotic areas were quantified using ImageJ and expressed as a percentage of total cortical area. Paraffin-embedded kidney sections (4 μm) from UUO and control mice were deparaffinized in xylene and rehydrated through a graded ethanol series. For antigen retrieval, slides were incubated in citrate buffer (pH 6.0) at 95 °C for 20 min. Endogenous peroxidase activity was quenched using 3% hydrogen peroxide for 10 min at room temperature (RT). Immunohistochemical staining was performed using UltraVision LP Detection System HRP polymer (Thermo Scientific, TL-060-HL) according to the manufacturer's recommended protocol. Briefly, slides were blokced using Ultraviosion Block for 5 min at RT, and then incubated with the following primary antibodise overnight at RT: collagen type 1 (1:200, Abcam, ab138492), PAI-1 (1:200, Invitrogen, PA5–119817, Carlsbaed, CA, USA), fibronectin (1:200, Abcam, ab2413), α-SMA (1:300, BD Biosciences, 610620,), and p-Smad3 (1:200, Cell Signaling, 9520)). After washing, Primary Antibody Enhancer was applied for 10 min at RT, followed by the HRP polymer for 15 min at RT. Visualization was achieved using DAB (Sigma-Aldrich, D4418) as the chromogen. Sections were counterstained with hematoxylin, dehydrated, and mounted. Positive staining was visualized under a light microscope (Leica Microsystem, Wetzlar, Germany) using Leica Application Suite V3.8 software (Leica Microsystems), and five randomly selected non-overlapping fields from the cortex were imaged per slide. Quantification of Sirius Red (collagen fiber, red) and immunostaining (brown color) positive areas was performed using computer-based morphometric analysis.

2.9. Statistical analysis

All data are presented as mean ± standard deviation. Statistical significance was determined using one-way analysis of variance followed by Student's *t*-test (Excel, Microsoft). A *p*-value <0.05 was considered statistically significant.

3. Results

3.1. Toxicity test of MHH

To assess the potential cytotoxicity of MHH, NRK-49F cells were treated with MHH at concentrations ranging from 1 to 10 μM for 24 h. MHH at 0.5–5 μM maintained cell viability above 80%, whereas MHH at

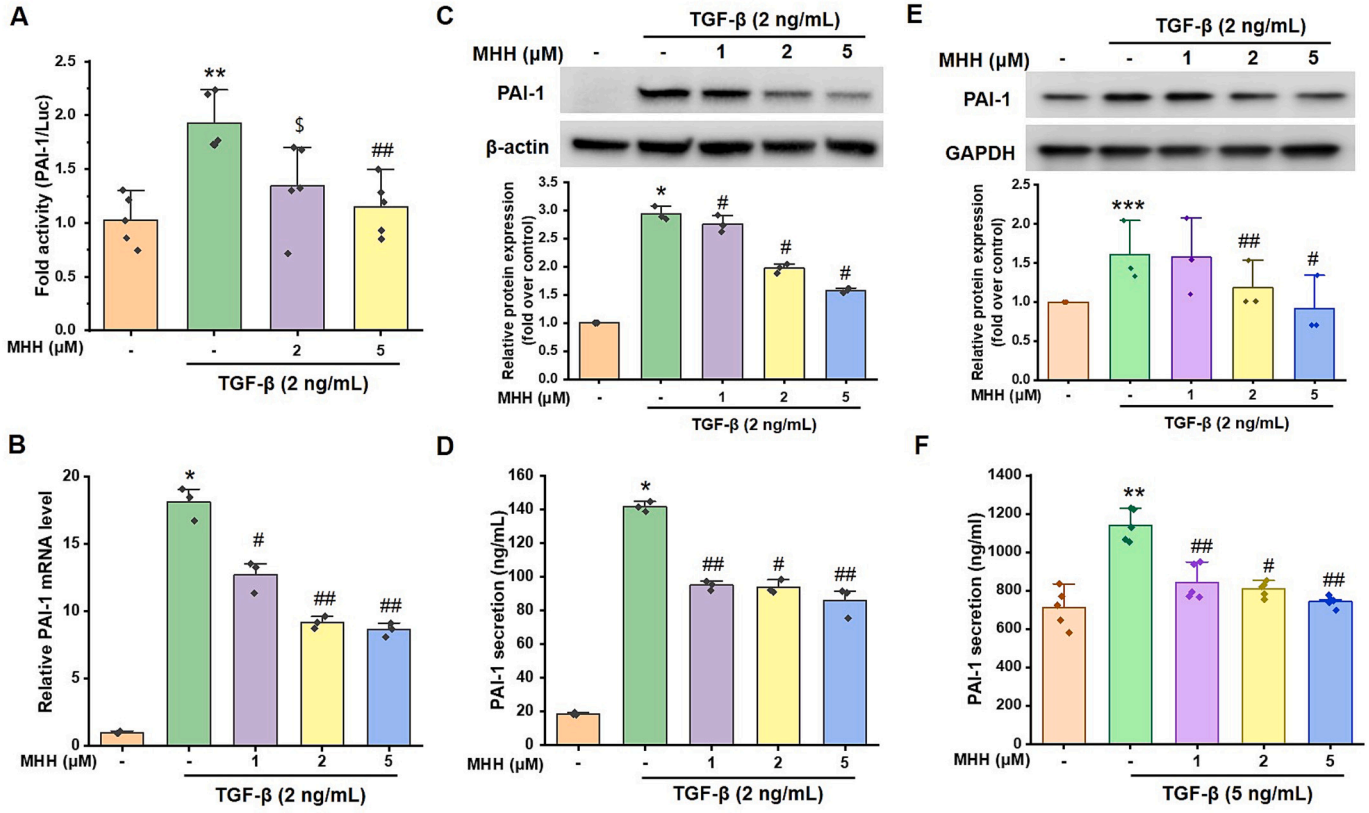

Fig. 1. Effects of MHH on TGF-β1-induced PAI-1 transcriptional activity and expression in renal cells. (A) Luciferase reporter assay of PAI-1 promoter activity. Serum-starved NRK-49F cells were transfected with PAI-1 promoter (−840 PAI-1 promoter Luc, 300 ng) for 4 h. Transfected cells were incubated in medium containing 0.5% FBS for 24 h and then treated with TGF-β1 (2 ng/mL) in the presence or absence of MHH (2 and 5 μM) for 24 h. (B) Real-time qPCR analysis of PAI-1 mRNA expression. GAPDH mRNA was used as an internal control. (C, E) Western blot analysis of PAI-1 protein expression. For real-time qPCR and western blot analysis, NRK-49F cells (C) or renal glomerular endothelial cells (E) were serum-starved with medium containing 0.5% FBS for 24 h and then treated with TGF-β1 (2 ng/mL) with or without MHH (0–5 μM) for 24 h. (D, F) ELISA analysis of secreted PAI-1 levels. NRK-49F cells (D) or renal glomerular endothelial cells (F) were serum-starved with medium containing 0.5% FBS for 24 h and then treated with TGF-β1 (2 or 5 ng/mL) with or without MHH (0–5 μM) for 24 h. Data are presented as mean ± SEM from three independent experiments. *$P < 0.001$, **$P < 0.01$ and ***$P < 0.05$ vs. control (−), #P < 0.001, ##P < 0.01 and $P < 0.05 vs. TGF-β1.

10 μM reduced it below 80% in NRK-49F cells (Fig. S1). Therefore, 1 to 5 μM MHH was used in all subsequent in vitro experiments.

3.2. MHH inhibited TGF-β1-induced PAI-1 secretion and expression

PAI-1 plays a crucial role in kidney fibrosis through its central function in regulating ECM remodeling and degradation (Chia et al., 2024; Lee et al., 2024; Lee and Ha, 2005; Ye et al., 2023). During drug screening, we discovered that MHH inhibited TGF-β1-induced PAI-1 secretion in several renal cell types. To determine whether MHH regulates PAI-1 at the transcriptional and translational levels, we first performed a transient transfection assay. MHH treatment significantly inhibited TGF-β1-induced PAI-1 promoter activity (Fig. 1A). Furthermore, we observed that MHH suppressed TGF-β1-stimulated PAI-1 mRNA and protein expression, as well as its secretion, in NRK-49F cells (Fig. 1B-D). These findings indicate that the downregulation of TGF-β1-induced transcriptional activation contributes to MHH-mediated inhibition of PAI-1. Given that PAI-1 is predominantly synthesized and released by renal endothelial cells, we extended our investigation to examine the effect of MHH on glomerular endothelial cells. Consistent with our previous observation, MHH significantly inhibited TGF-β1-stimulated PAI-1 protein expression and its subsequent secretion in these cells (Fig.1E and F). These data confirm that the inhibitory effect of MHH is not limited to fibroblasts but also extends to the vascular components of the kidney.

3.3. MHH suppressed TGF-β1-induced mRNA and protein expression of renal fibrotic markers

As a central mediator of renal fibrosis, TGF-β1orchestrates the upregulation of various profibrotic factors, including collagen type I, fibronectin, and α-SMA (Ma and Meng, 2019; Ren et al., 2023; Zou et al., 2025). We therefore investigated whether MHH could regulate TGF-β1-mediated fibrogenic response in NRK-49F cells. Real-time q-PCR analysis revealed that MHH treatment dose-dependently attenuated the TGF-β1-induced mRNA expression of collagen type I, fibronetin, and α-SMA (Fig. 2A-C). Consistent with these transcriptional changes, MHH significantly inhibited the protein expression of these markers in TGF-β1-stimulated fibroblasts (Fig. 2D-G). These results indicate that MHH effectively interferes with the synthesis of key extracellular matrix components and myofibroblast activation markers.

3.4. MHH attenuated UUO-induced tubular atrophy and interstitial fibrosis

To evaluate the anti-fibrotic potential of MHH in vivo, we employed the UUO model. MHH was orally administered to mice both prior to and following the ligation of the left ureter. At 10 post-obstruction, the vehicle-treated UUO group exhibited pronounced tubular atrophy and extensive interstitial fibrosis. However, histological analysis via H&E and Sirius Red staining demonstrated that MHH treatment significantly attenuated renal structural deterioration and diminished collagen accumulation (Fig. 3).

3.5. MHH reduced UUO-induced expression of renal fibrotic factors

Immunohistochemical analysis demonstrated that UUO triggered a robust upregulation of PAI-1, collagen type I, fibronection, and α-SMA within the kidneys of the vehicle-treated UUO group. In contrast, MHH administration significantly attenuated the expression of both PAI-1 and these associated profibrotic markers (Fig. 4). These histological findings were further corroborated by molecular analysis; as shown in Fig. 5, the mRNA and protein levels of these fibrotic markers were markedly elevated in vehicle-treated UUO kidneys, whereas MHH treatment

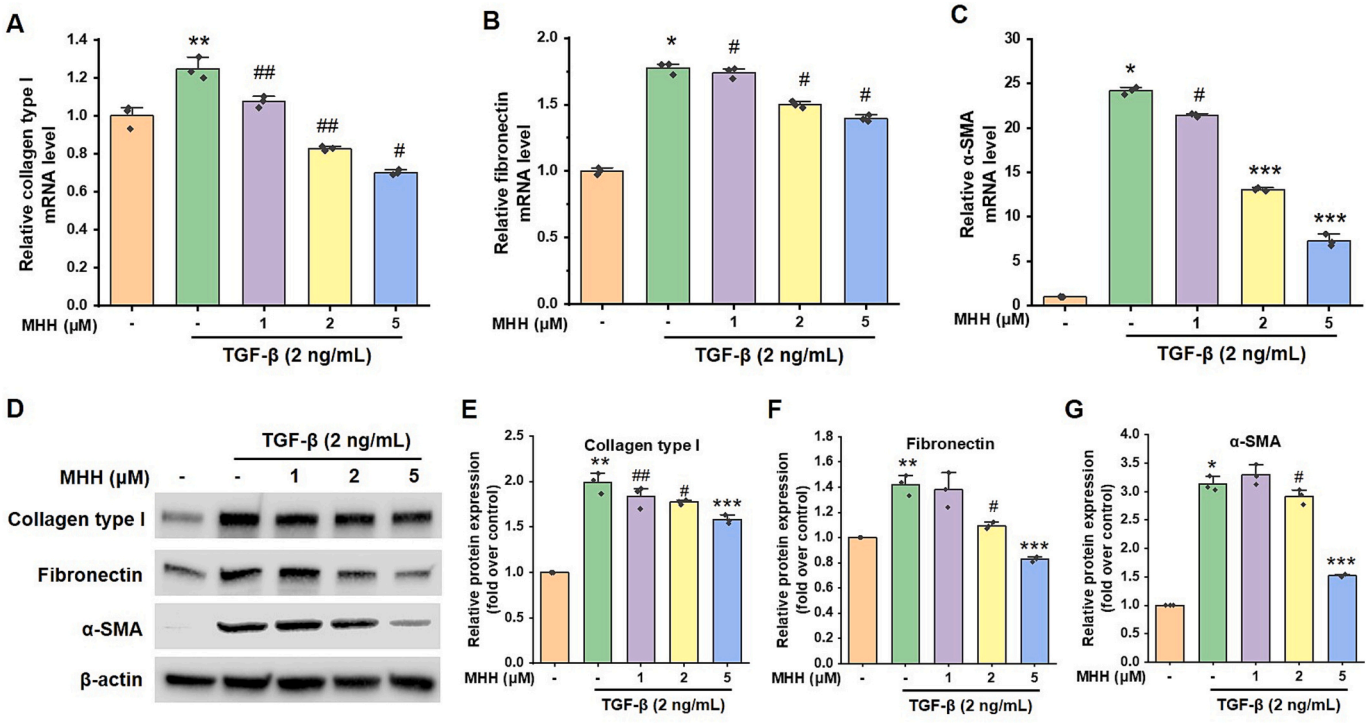

Fig. 2. Effects of MHH on TGF-β1-induced mRNA expression and protein level of renal fibrotic markers in NRK-49F cells. NRK-49F cells were serum-starved with medium containing 0.5% FBS for 24 h and then treated with TGF-β1 (2 ng/mL) with or without MHH (0–5 μM) for 24 h. (A–C) Real-time qPCR analysis of mRNA expression of collagen type I, fibronectin, and α-SMA in NRK-49F cells treated with or without TGF-β1 and MHH. GAPDH mRNA was used as an internal control. *P < 0.001 and **P < 0.05 vs. control (−), ***P < 0.001 and #P < 0.01 and ##P < 0.05 vs. TGF-β1. (D-G) Western blot and quantification analysis of protein expression of collagen type I (E), fibronectin (F), and α-SMA (G) in NRK-49F cells treated with or without TGF-β1 and MHH. Data are presented as mean ± SEM from three independent experiments. *P < 0.001 and **P < 0.01 vs. control (−), and ***P < 0.001, #P < 0.01 and ##P < 0.05 vs. TGF- β1.

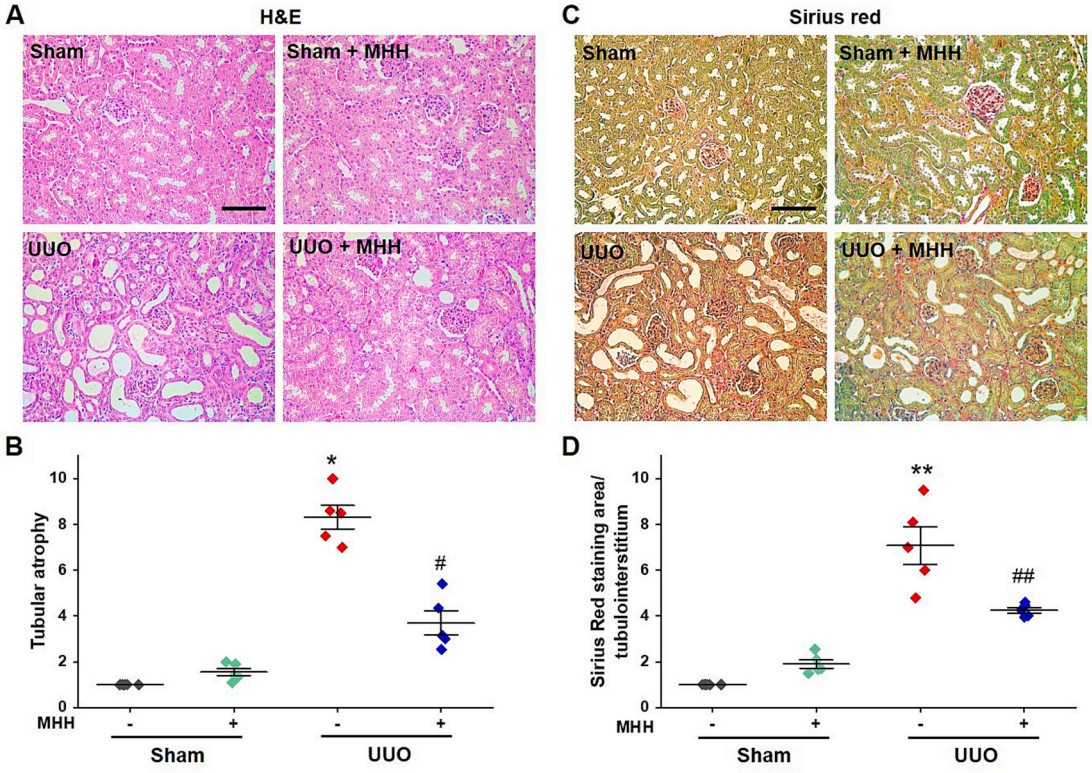

Fig. 3. Effects of MHH on UUO-induced tubular atrophy and interstitial fibrosis. Mice in the MHH groups were received oral gavage of MHH (5 mg/kg/day) for 5 days prior to UUO surgery. Administration continued for 10 days post-surgery until sacrifice. Sham groups received equivalent volumes of the vehicle on the same schedule ($n = 7$ in each group). (A, C) Representative images of kidney sections from the vehicle- or MHH-treated group stained with H&E (A) and Sirius Red (C) at 20× magnification (Scale bar = 100 μm). (B, D) Quantitative analysis of tubular injury scores (B) and kidney fibrotic areas (D) performed using computer-assisted morphometric analysis in the UUO model. Values were normalized to the sham group and presented as fold change relative to the control (=1). Data are presented as mean ± SEM from five independent measurements. *P < 0.01 and **P < 0.05 vs. Sham, and #P < 0.01 and ##P < 0.05 vs. UUO (−). (For interpretation of the references to color in this figure legend, the reader is referred to the web version of this article.)

consistently downregulated their expression. Collectively, these in vivo findings indicate that MHH effectively protects against obstruction-induced renal fibrogenesis.

3.6. MHH inhibited Smad3 phosphorylation in vitro and in vivo

TGF-β orchestrates the expression of fibrogenic factors and extracellular matrix proteins via Smad-dependent signaling, ultimately driving myofibroblast activation and tubulointerstitial fibrosis. To elucidate the molecular mechanism underlying the anti-fibrotic effects of MHH, we investigated its impact on Smad3 phosphorylation both in vitro and in vivo. MHH treatment significantly suppressed TGF-β1-induced Smad3 phosphorylation in NRK-49F cells (Fig. 6A). Consistent with these cellular findings, MHH administration markedly attenuated Smad3 phosphorylation in the obstructed kidneys of the UUO model (Fig. 6B). Taken together, these results suggest that MHH exerts its antifibrotic activity by inhibiting the canonical TGF-β1/Smad3 signaling pathway.

4. Discussion

Here, we demonstrate for the first time that MHH, an anticholinergic drug (Scott and Njardarson, 2019), previously used for neurological disorders, exerts potent antifibrotic effects in both in vitro and in vivo models of renal fibrosis. Our findings indicate that MHH primarily attenuates fibrosis by inhibiting the TGF-β1/Smad3 signaling pathway, which is well-established as a central driver of renal fibrogenesis.

We confirmed that MHH was safe in renal fibroblasts, as it did not affect cell viability at concentrations up to 5 μM, establishing a foundation for potential repurposing without cytotoxicity in kidney cells. We administered a dose of 5 mg/kg in the UUO model. Notably, this concentration effectively mitigated renal fibrosis without inducing any observable adverse effects or systemic toxicity in the mice, suggesting a favorable safety profile for MHH at this therapeutic dosage. Previous preclinical studies have reported an effective range of 2 to 5 mg/kg specifically optimized for evaluating anticholinergic activity.

TGF-β1, a key mediator of fibrotic progression, plays a central role in inducing cellular phenotypic shifts that ultimately lead to the formation of myofibroblasts (Ren et al., 2023). During the progression of renal fibrosis, the production of various inflammatory cytokines, most notably TGF-β1, is markedly elevated (Black et al., 2019). Concurrently, excessive deposition of ECM components, including PAI-1, collagen type I, fibronectin, and α-SMA, occurs within the renal interstitium (Lee et al., 2024; Wight and Potter-Perigo, 2011). As renal fibrosis progresses, resident renal interstitial mesenchymal cells diminish in number, while a subset undergoes phenotypic transition into myofibroblasts (Meran and Steadman, 2011).

Following TGF-β1 stimulation, NRK-49F cells showed marked upregulation of PAI-1, a critical profibrotic mediator that inhibits ECM degradation and promotes matrix accumulation (Huang et al., 2008; Yu et al., 2003). MHH treatment significantly suppressed both *PAI-1* gene expression and protein levels, as well as secretion, indicating its regulatory role in extracellular matrix remodeling. In addition to PAI-1, MHH effectively downregulated the expression of canonical fibrotic markers, including collagen type I, fibronectin, and α-SMA, at both the transcriptional and protein levels. This suggests that MHH interferes with fibroblast activation and myofibroblast differentiation, two key processes in the progression of renal fibrosis.

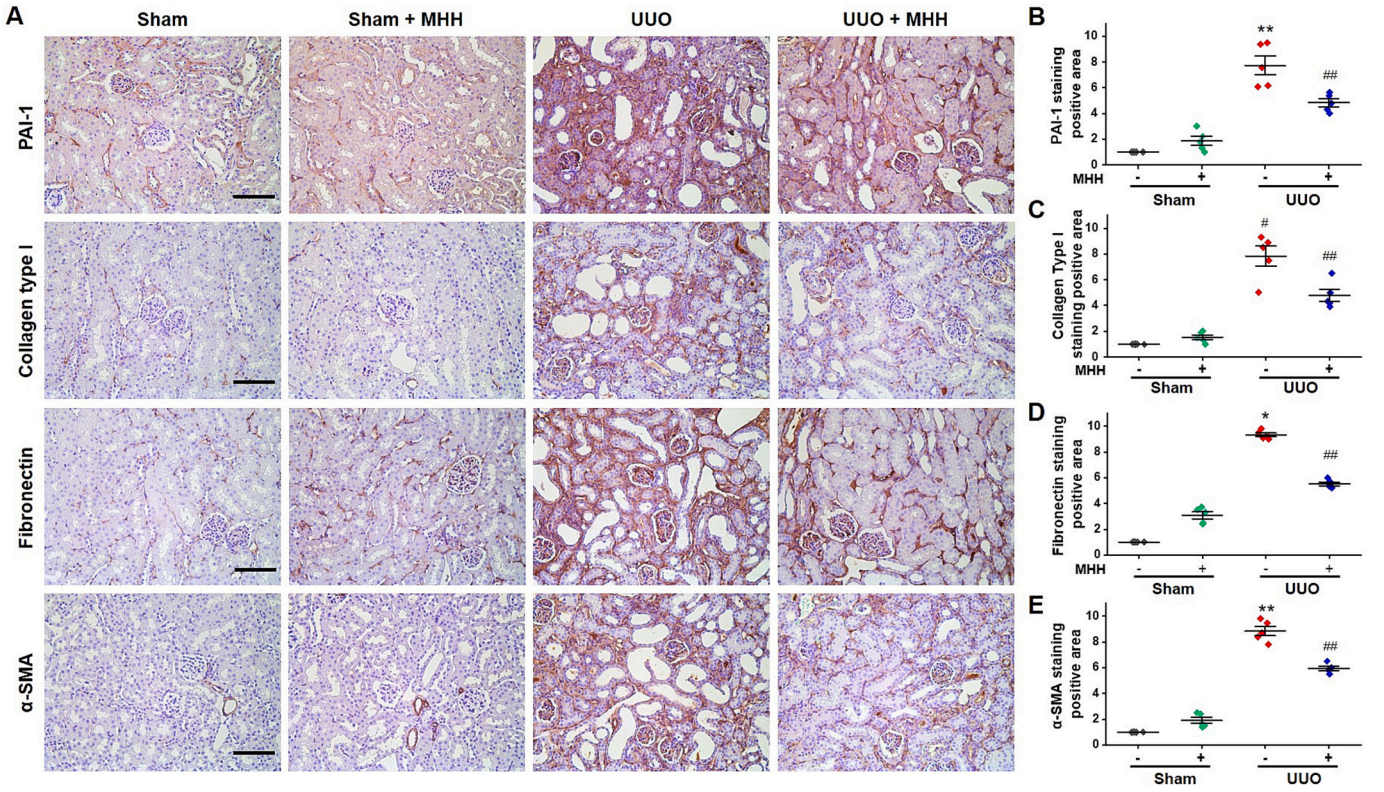

Fig. 4. Effects of MHH on UUO-induced expression of renal fibrotic markers. Mice in the MHH groups were received oral gavage of MHH (5 mg/kg/day) for 5 days prior to UUO surgery. Administration continued for 10 days post-surgery until sacrifice. Sham groups received equivalent volumes of the vehicle on the same schedule (n = 7 in each group). (A) Representative immunohistochemical staining images for PAI-1, collagen type I, fibronectin, and α-SMA in kidney tissues from the vehicle- or MHH-treated UUO group. Images were captured at 200× magnification (Scale bar = 100 μm). (B–E) Quantitative morphometric analysis of the positively stained areas for each marker. Data were analyzed using computer-assisted software. Values were normalized to the sham group and presented as fold change relative to the control (=1). Data are presented as mean ± SEM from five independent measurements. *P < 0.001, **P < 0.01 and #P < 0.05 vs. Sham, and ##P < 0.05 vs. UUO (−).

The experimental UUO mouse model is widely employed to provoke renal tubulointerstitial fibrosis and serves as a representative system for studying human chronic obstructive nephropathy, a condition characterized by rapid disease progression (Lee et al., 2024; Martínez-Klimova et al., 2019). In vivo study revealed that MHH administration markedly attenuated tubular atrophy and collagen deposition in the obstructed kidneys of UUO mice. In addition, expression levels of fibrogenic genes and proteins were substantially decreased in the kidneys of MHH-treated mice compared with untreated UUO controls. These results clearly establish the protective role of MHH against obstructive renal injury.

Mechanistically, our data reveal that MHH suppresses TGF-β1-induced Smad3 phosphorylation in both NRK-49F cells and obstructed kidneys of UUO mice. Smad3 is a key transcription factor mediating the profibrotic effects of TGF-β1 through promoting ECM gene transcription and myofibroblast activation (Flanders, 2004; Li et al., 2024). The inhibition of Smad3 phosphorylation thus provides a mechanistic basis for the antifibrotic effects of MHH observed in this study.

MHH is an anticholinergic and antiparkinsonian agent. A recent study by Fares et al. reported that MHH exerted antitumor activity against metastatic breast cancer, including brain metastases, suggesting its potential for drug repurposing in oncology (Fares et al., 2023). Our findings indicate that MHH holds promise as a drug repositioning candidate for treating renal disease by suppressing renal fibrogenic factors and ECM accumulation through modulation of the TGF-β1/Smad3 signaling pathway. A growing body of evidence suggests that various natural products can mitigate renal fibrosis by targeting multiple signaling cascades, including inflammatory, oxidative stress, and TGF-β/Smad pathways (Chung et al., 2022; Feng et al., 2025; Hwang et al., 2024; Guo et al., 2024; Wang et al., 2021). Although these compounds are often suitable for long-term administration due to their low toxicity, their clinical utility is frequently hindered by poor bioavailability and challenges in the standardization of active components. In contrast, Metixene hydrochloride hydrate (MHH) presents a more viable therapeutic strategy for fibrotic nephropathy. As an FDA-approved agent with a well-established safety profile, MHH circumvents the pharmacological limitations associated with unrefined natural products, offering a more direct and standardized approach to renal protection. Furthermore, these findings demonstrate that MHH can be positioned as a novel candidate for drug repurposing in the treatment of chronic renal fibrosis, particularly for diabetic nephropathy.

The clinical significance of our findings lies in the potent suppression of PAI-1 by MHH across multiple renal cell types. Elevated PAI-1 levels are strongly associated with poor renal prognosis in CKD patients. Therefor, the ability of MHH downregulate PAI-1 at both the transcriptional and translational levels suggests its potential as a targeted anti-fibrotic therapy. Furthermore, the potent inhibition of Smad3 phosphorylation by MHH indicates a direct modulates of key pathway in renal fibrogenesis, offering a distinct pharmacological advantage over conventional therapies that primarily target systemic hemodynamics.

Despite these important findings, this study has several limitations that warrant further investigation. First, while our study focused on the canonical TGF-β1/Smad3 pathway, renal fibrosis involves multiple signaling pathways, and the possible involvement of other pathways should be elucidated through further studies. Second, while the UUO model allows for rapid and robust assessment of fibrogenesis, it may not fully reflect the chronic and progressive clinical conditions such as diabetic nephropathy. Third, although oral administration of MHH showed effective, our study did not evalute the comprehensive

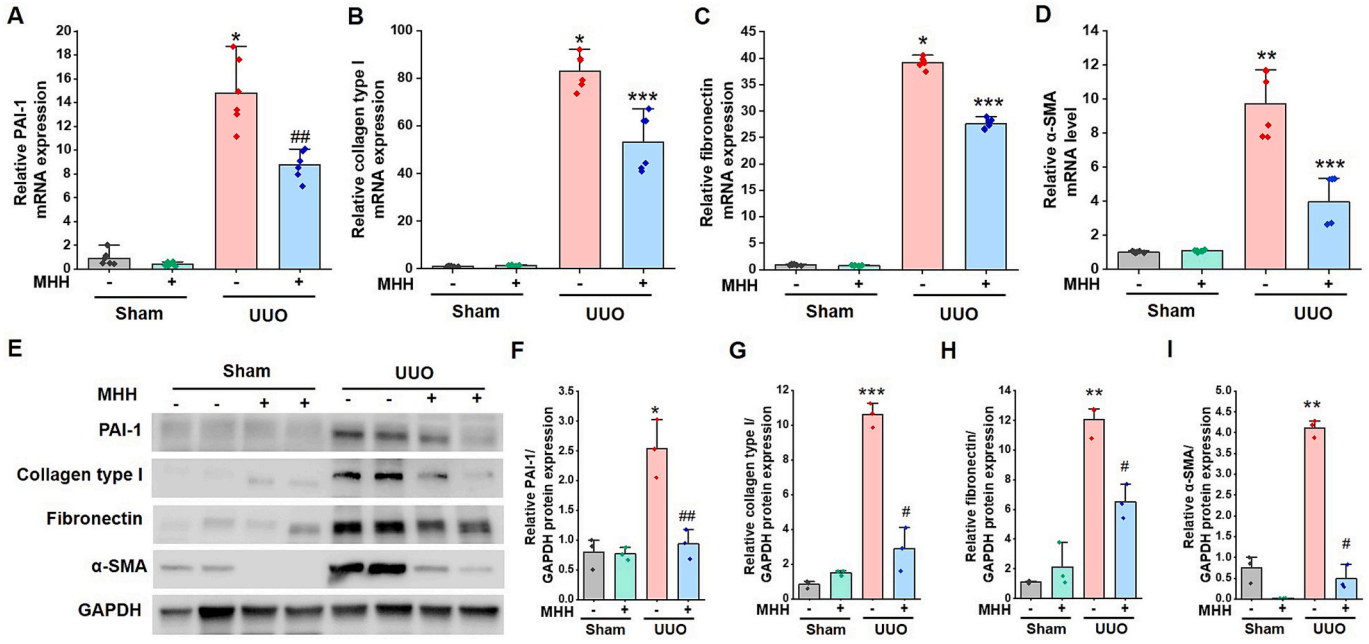

Fig. 5. Effects of MHH on UUO-induced gene and protein expression of renal fibrotic markers. Mice in the MHH groups were received oral gavage of MHH (5 mg/kg/day) for 5 days prior to UUO surgery. Administration continued for 10 days post-surgery until sacrifice. Sham groups received equivalent volumes of the vehicle on the same schedule (n = 7 in each group). (A-D) Real-time qPCR analysis of mRNA expression of PAI-1 (A), collagen type I (B), fibronectin (C), and α-SMA (D) in kidney tissues from the vehicle- or MHH-treated UUO group. GAPDH was used as an internal control. ($n = 6$) (E) Representative western blot showing the protein expression of PAI-1, collagen type I, fibronectin, α-SMA, and GAPDH in kidney tissues from the vehicle- or MHH-treated UUO group. (F—I) Densitometric quantification of PAI-1 (F), collagen type I (G), fibronectin (H), and α-SMA (I). Protein levels were normalized to GAPDH and expressed as fold change relative to the sham group (=1). Data are presented as mean ± SEM from three independent experiments. *P < 0.05, **P < 0.01 and ***P < 0.001 vs Sham, and #P < 0.01 and ##P < 0.001 vs UUO (−).*P < 0.01 and **P < 0.001 vs. Sham, and ***P < 0.01 and #P < 0.001 vs UUO (−).

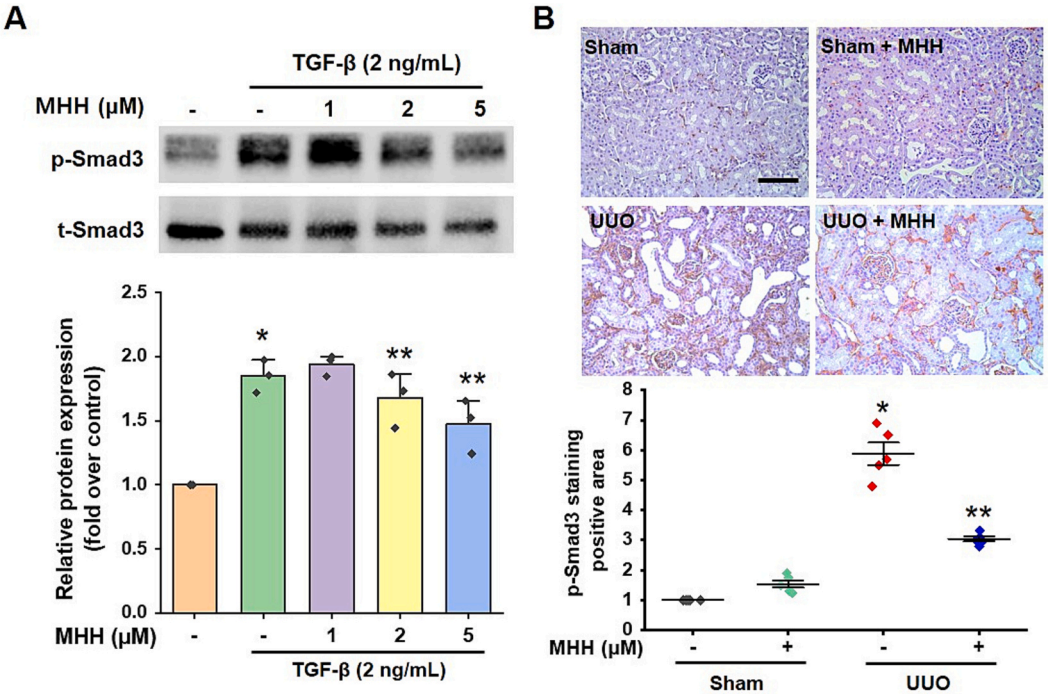

Fig. 6. Effects of MHH on Smad3 phosphorylation in vivo and in vitro. (A) Representative western blot analysis showing the protein expression of phospho-Smad3 (p-Smad3) in NRK-49F cells treated with or without TGF-β1 and MHH. Protein levels were normalized to total-Smad3 (t-Smad3) and expressed relative to control (=1). Data are presented as mean ± SEM from three independent experiments. (B) Representative immunohistochemical staining images for p-Smad3 in kidney tissues from the vehicle- or MHH-treated UUO group. Images were captured at 200× magnification (Scale bar = 100 μm). Quantitative morphometric analysis of p-Smad3-positive areas. Data were analyzed using computer-assisted software. Values were normalized to the sham group and presented as fold change relative to the control (=1). Data are presented as mean ± SEM from five independent measurements. *P < 0.01 vs. control (−), and **P < 0.05 vs. TGF-β1.

pharmacokinetics and long-term systemic safety of MHH. Future study utilizing cell-specific knockout models and various chronic kidney disease models are essential to translate these findings into clinical practice.

5. Conclusion

Our study demonstrates that MHH, a previously approved anticholinergic drug (Scott and Njardarson, 2019), exerts significant antifibrotic effects through inhibition of the TGF-β1/Smad3 signaling pathway in both NRK-49F kidney fibroblasts and UUO-induced renal fibrosis models. MHH effectively attenuated renal structural damage and ECM accumulation in vivo, while suppressing the expression of key fibrotic factors, including collagen type I, PAI-1, fibronectin, and α-SMA. These results suggest the potential of MHH as a repositioned therapeutic candidate for CKD. However, further preclinical and clinical studies are warranted to confirm its efficacy and safety in human CKD, thereby providing more robust evidence for its clinical application.

CRediT authorship contribution statement

Kyeong-Min Lee: Writing – review & editing, Writing – original draft, Visualization, Validation, Supervision, Software, Methodology, Funding acquisition, Formal analysis, Conceptualization. **Yeo Jin Hwang:** Visualization, Validation, Software, Methodology, Investigation, Conceptualization.

Declaration of generative AI and AI-assisted technologies in the writing process

During the preparation of this work, the authors used OpenAI's GPT-5 plus or Gemini Pro in order to improve grammar and spelling. After using this tool, the authors reviewed and edited the content as needed and take full responsibility for the content of the publication.

Funding

This study was supported by DGIST projects 26-NT-01 and NRF-2021R1A2C1011314 from the National Research Foundation of Korea, funded by the Ministry of Science, ICT of the Republic of Korea.

Declaration of competing interest

The authors declare that they have no known competing financial interests or personal relationships that could have appeared to influence the work reported in this paper.

Appendix A. Supplementary data

Supplementary data to this article can be found online at https://doi.org/10.1016/j.yexmp.2026.105025.

Data availability

Data will be made available on request.

References

Black, L.M., et al., 2019. Renal inflammation and fibrosis: a double-edged sword. J. Histochem. Cytochem. 67, 663–681. https://doi.org/10.1369/0022155419852932.

Chia, Z.J., et al., 2024. Transforming growth factor-β receptors: versatile mechanisms of ligand activation. Acta Pharmacol. Sin. 45, 1337–1348. https://doi.org/10.1038/s41401-024-01235-6.

Chung, J.Y., et al., 2022. AANG prevents Smad3-dependent diabetic nephropathy by restoring pancreatic β-cell development in db/db mice. Int. J. Biol. Sci. 18, 5489–5502. https://doi.org/10.7150/ijbs.72977.

Duff, R., et al., 2024. Global health inequalities of chronic kidney disease: a meta-analysis. Nephrol. Dial. Transplant. 39, 1639–1709. https://doi.org/10.1093/ndt/gfae048.

Fares, J., et al., 2023. Metixene is an incomplete autophagy inducer in preclinical models of metastatic cancer and brain metastases. J. Clin. Invest. 133, e161142. https://doi.org/10.1172/JCI161142.

Feng, X., et al., 2023. Secular trends of epidemiologic patterns of chronic kidney disease over three decades: an updated analysis of the global burden of disease study 2019. BMJ Open 13, e064540. https://doi.org/10.1136/bmjopen-2022-064540.

Feng, H.Y., et al., 2025. Anthraquinones from *Rheum officinale* ameliorate renal fibrosis in acute kidney injury and chronic kidney disease. Drug Des. Devel. Ther. 19, 5739–5760. https://doi.org/10.2147/DDDT.S521265.

Flanders, K.C., 2004. Smad3 as a mediator of the fibrotic response. Int. J. Exp. Pathol. 85, 47–64. https://doi.org/10.1111/j.0959-9673.2004.00377.x.

Gagliardini, E., Benigni, A., 2007. Therapeutic potential of TGF-β inhibition in chronic renal failure. Expert. Opin. Biol. Ther. 7, 293–304. https://doi.org/10.1517/14712598.7.3.293.

Gifford, C.C., et al., 2021. Negative regulators of TGF-β1 signaling in renal fibrosis; pathological mechanisms and novel therapeutic opportunities. Clin. Sci. 135, 275–303. https://doi.org/10.1042/cs20201213.

Gu, Y.Y., et al., 2024. Therapeutic potential for renal fibrosis by targeting Smad3-dependent noncoding RNAs. Mol. Ther. 32, 313–324. https://doi.org/10.3389/fphys.2015.00082.

Guo, Z.Y., et al., 2024. Poria cocos: traditional uses, triterpenoid components and their renoprotective pharmacology. Acta Pharmacol. Sin. 46, 836–851. https://doi.org/10.1038/s41401-024-01404-7.

Guo, J., et al., 2025. The global, regional, and national patterns of change in the burden of chronic kidney disease from 1990 to 2021. BMC Nephrol. 26, 136. https://doi.org/10.1186/s12882-025-04028-z.

Hill, N.R., et al., 2016. Global prevalence of chronic kidney disease - a systematic review and Meta-analysis. PLoS One 11, e0158765. https://doi.org/10.1371/journal.pone.0158765.

Hodgkins, K.S., Schnaper, H.W., 2012. Tubulointerstitial injury and the progression of chronic kidney disease. Pediatr. Nephrol. 27, 901–909. https://doi.org/10.1007/s00467-011-1992-9.

Huang, W., et al., 2008. Aldosterone and TGF-β1 synergistically increase PAI-1 and decrease matrix degradation in rat renal mesangial and fibroblast cells. Am. J. Physiol. Renal Physiol. 294, F1287–F1295. https://doi.org/10.1152/ajprenal.00017.2008.

Huang, R., et al., 2023. Kidney fibrosis: from mechanisms to therapeutic medicines. Signal Transduct. Target. Ther. 8, 129. https://doi.org/10.1038/s41392-023-01379-7.

Hwang, Y.J., et al., 2024. Alantolactone alleviates epithelial-mesenchymal transition by regulating the TGF-beta/STAT3 signaling pathway in renal fibrosis. Heliyon 10, e36253. https://doi.org/10.1016/j.heliyon.2024.e36253.

Jung, G.S., et al., 2020. Lin28a attenuates TGF-β-induced renal fibrosis. BMB Rep. 53, 594–599. https://doi.org/10.5483/BMBRep.2020.53.11.153.

Lee, H.B., Ha, H., 2005. Plasminogen activator inhibitor-1 and diabetic nephropathy. Nephrology (Carlton) 10 (Suppl), S11–S13. https://doi.org/10.1111/j.1440-1797.2005.00449.x.

Lee, K.M., et al., 2024. Alantolactone attenuates renal fibrosis via inhibition of transforming growth factor β/Smad3 Signaling pathway. Diabetes Metab. J. 48, 72–82. https://doi.org/10.4093/dmj.2022.0231.

Levey, A.S., Coresh, J., 2011. Chronic kidney disease. Lancet 379, 165–180. https://doi.org/10.1016/S0140-6736(11)60178-5.

Li, Y.Y., Jones, S.J.M., 2012. Drug repositioning for personalized medicine. Genome Med. 4, 27. https://doi.org/10.1186/gm326.

Li, L., et al., 2022. The fibrogenic niche in kidney fibrosis: components and mechanisms. Nat. Rev. Nephrol. 18, 545–557. https://doi.org/10.1038/s41581-022-00590-z.

Li, J., et al., 2024. TGF-β/Smad signaling in chronic kidney disease: exploring post-translational regulatory perspectives (review). Mol. Med. Rep. 30. https://doi.org/10.3892/mmr.2024.13267.

Lv, J.-C., Zhang, L.-X., 2019. Prevalence and Disease Burden of Chronic Kidney Disease. Renal Fibrosis: Mechanisms and Therapies, pp. 3–15. https://doi.org/10.1007/978-981-13-8871-2_1.

Ma, T.-T., Meng, X.-M., 2019. TGF-β/Smad and renal fibrosis. In: Liu, B.-C., et al. (Eds.), Renal Fibrosis: Mechanisms and Therapies. Springer Singapore, Singapore, pp. 347–364. https://doi.org/10.1007/978-981-13-8871-2_16.

Martínez-Klimova, E., et al., 2019. Unilateral ureteral obstruction as a model to investigate fibrosis-attenuating treatments. Biomolecules 9. https://doi.org/10.3390/biom9040141.

Meran, S., Steadman, R., 2011. Fibroblasts and myofibroblasts in renal fibrosis. Int. J. Exp. Pathol. 92, 158–167. https://doi.org/10.1111/j.1365-2613.2011.00764.x.

Orr, S.E., Bridges, C.C., 2017. Chronic kidney disease and exposure to nephrotoxic metals. Int. J. Mol. Sci. 18, 1039. https://doi.org/10.3390/ijms18051039.

Ren, L.L., et al., 2023. TGF-beta as a master regulator of aging-associated tissue fibrosis. Aging Dis. 14, 1633–1650. https://doi.org/10.14336/AD.2023.0222.

Ruiz-Ortega, M., et al., 2020. Targeting the progression of chronic kidney disease. Nat. Rev. Nephrol. 16, 269–288. https://doi.org/10.1038/s41581-019-0248-y.

Scott, K.A., Njardarson, J.T., 2019. Analysis of US FDA-approved drugs containing Sulfur atoms. In: Jiang, X. (Ed.), Sulfur Chemistry. Springer International Publishing, Cham, pp. 1–34. https://doi.org/10.1007/978-3-030-25598-5_1.

Sobreiro-Almeida, R., et al., 2021. Renal regeneration: the role of extracellular matrix and current ECM-based tissue engineered strategies. Adv. Healthc. Mater. 10, 2100160. https://doi.org/10.1002/adhm.202100160.

Wang, J., et al., 2021. Puerarin alleviates UUO-induced inflammation and fibrosis by regulating the NF-κB P65/STAT3 and TGFβ1/Smads signaling pathways. Drug Des. Devel. Ther. 15, 3697–3708. https://doi.org/10.2147/DDDT.S321879.

Wight, T.N., Potter-Perigo, S., 2011. The extracellular matrix: an active or passive player in fibrosis? Am. J. Physiol. Gastrointest. Liver Physiol. 301, G950–G955. https://doi.org/10.1152/ajpgi.00132.2011.

Würth, R., et al., 2016. Drug-repositioning opportunities for cancer therapy: novel molecular targets for known compounds. Drug Discov. Today 21, 190–199. https://doi.org/10.1016/j.drudis.2015.09.017.

Yu, L., et al., 2003. TGF-β isoforms in renal fibrogenesis. Kidney Int. 64, 844–856. https://doi.org/10.1046/j.1523-1755.2003.00162.x.

Zhang, Y., et al., 2018. The preventive and therapeutic implication for renal fibrosis by targetting TGF-β/Smad3 signaling. Clin. Sci. 132, 1403–1415. https://doi.org/10.1042/cs20180243.

Zou, Y., et al., 2025. Role of the TGF-β/Smad signaling pathway in the transition from acute kidney injury to chronic kidney disease (review). Int. J. Mol. Med. 56 (4), 162. https://doi.org/10.3892/ijmm.2025.5603.